Influence of Microstructure on IASCC Growth Behavior of Neutron Irradiated Type 304 Austenitic Stainless Steels in Simulated BWR Condition

Yoshiyuki Kaji*[1], Yukio Miwa[1], Akira Shibata[1], Junichi Nakano[1], Takashi Tsukada[1], Kenichi Takakura[2], Kiyotomo Nakata[2]

[1]Japan Atomic Energy Agency (JAEA), Tokai-mura, Ibaraki, 319-1195, Japan

[2]Japan Nuclear Energy Safety Organization (JNES), Toranomon, Minato-ku, 105-0001, Tokyo, Japan

kaji.yoshiyuki@jaea.go.jp

***Abstract*- Crack growth rate (CGR) tests have been conducted with neutron irradiated compact tension (CT) specimens. The specimens were irradiated in the core region of the Japan Materials Testing Reactor (JMTR) in simulated BWR water environments at 288 °C from 0.37 to 5.55 x 10^{25} n/m^2 (E>1MeV) (0.62-9.2dpa). The CGR tests were performed using the reversing DC potential drop (DCPD) method under constant load at a few average stress intensity factors (K) and electrochemical corrosion potential (ECP) conditions at 288 °C in water. The CGRs of base metals in high ECP condition with 10<K<30 MPam$^{1/2}$, increased with increasing neutron fluence until 2dpa and the CGRs were almost the same from 2dpa to 10dpa. We investigated the influence of microstructure on CGR by microstructure observation and local strain measurement around the precipitate. This paper will discuss the relationship between CGR and microstructure / radiation hardening / radiation induced segregation (RIS).**

Keywords- IASCC; CGR; Microstructure; Type 304 Stainless Steel; BWR

I. INTRODUCTION

Irradiation assisted stress corrosion cracking (IASCC) is one of the critical concerns as degradation of core internal components in light water reactors (LWRs) for a long period and recognized as the most important degradation phenomena affecting the integrity of both boiling water reactors (BWRs) and pressurized water reactors (PWRs) [1-8]. It takes the form of intergranular stress corrosion cracking (IGSCC) and the critical fluence level has been reported to be about 5x10^{24} n/m^2 in Type 304 stainless steel (SS) [1,4,7,8]. IASCC failures have been attributed to radiation hardening and radiation induced segregation (RIS) of impurities and/or alloying elements at grain boundaries. Many studies on IASCC have been conducted over the last two decades. However the mechanism of IASCC is not fully understood. Since practical engineering databases about IASCC are not sufficient to evaluate the structural integrity of core shroud, it is an urgent problem to prepare the experimental IASCC databases for aging management of the LWRs.

Japan Nuclear Energy Safety organization (JNES) has been conducting an IASCC project [9, 10] as a part of safety research and development study for the aging management and maintenance of the nuclear power plant. The objective of this project is to prepare an evaluation guide for the regulatory side, which uses it to evaluate the utility's aging management technical evaluation report. In the BWR study, the main target component is the core shroud and post irradiation experiments (PIEs) have been conducted to acquire the IASCC evaluation data including IASCC susceptibility, crack growth rate (CGR) and fracture toughness data. Especially, it is important to obtain CGR data from irradiated materials to support plant lifetime assessment of reactor components, but for which there are few data.

In this study, CGR data of neutron irradiated Type 304 SS are obtained as reference data. The CGR data of Type 304 SS will be discussed in terms of dependences of neutron fluence, applied stress and water chemistry, together with mechanical property, microstructure and microchemistry changes due to neutron irradiation.

II. EXPERIMENTAL PROCEDURE

A. Materials

The chemical compositions of the base metals are shown in Table 1. The chemical compositions of the prepared materials are similar to those of typical BWR core components. The heat treatment (1030 ^{o}Cx30 min W.Q.) diminished the enriched chromium (and molybdenum) concentration at grain boundaries of the as-received materials to simulate the new fusion line of the weld heat affected zone (HAZ).

TABLE I CHEMICAL COMPOSITIONS OF TEST MATERIALS

Material	C	Si	Mn	P	S	Ni	Cr	Mo	N	Co
Type 304 SS	0.05	0.65	1.20	0.024	0.004	8.93	18.58	-	-	0.04
Type 316L SS	0.008	0.43	0.83	0.023	0.001	12.55	17.54	2.11	-	0.02
Type 304L SS	0.009	0.58	0.85	0.020	0.001	9.78	18.43	-	-	0.05

Heat treatment condition: 1030^{o}C x 30min → Water Quench

Tensile tests were conducted in air at 288°C and Vickers hardness tests were carried out in air at room temperature. The microstructure of irradiated Type 304 and L-grade SS were observed with a field-emission gun transmission electron microscope (FEG-TEM), Hitachi HF-2000 with an acceleration voltage of 200 kV. The observations of microstructure were performed for each condition using bright-field, dark-field and weak-beam-dark-field imaging techniques. In order to measure the defect numbers and size, irradiation induced defects were observed near the foil edge, in regions with a thickness less than 100 nm, which minimizes overlap of defects and improves the accuracy of the measurements. Solute compositions near grain boundaries were analyzed by FEG-TEM with an energy dispersive x-ray spectrometer (EDS).

B. *Specimens*

The schematic of CT specimen is shown in Fig. 1. Sampling position of the CT specimen is shown in Fig. 2. 0.5T-CT specimens cut in the T-S orientation. The specimen has side grooves with 5 % depth of the thickness on each side surface. Prior to the irradiation in the high temperature water, a fatigue pre-crack with a length of about 1.5 mm (a/W=0.45) was introduced to the specimens by cyclic loading at room temperature in air. The maximum K values at the end of fatigue pre-cracks were adjusted to 12 MPam$^{1/2}$.

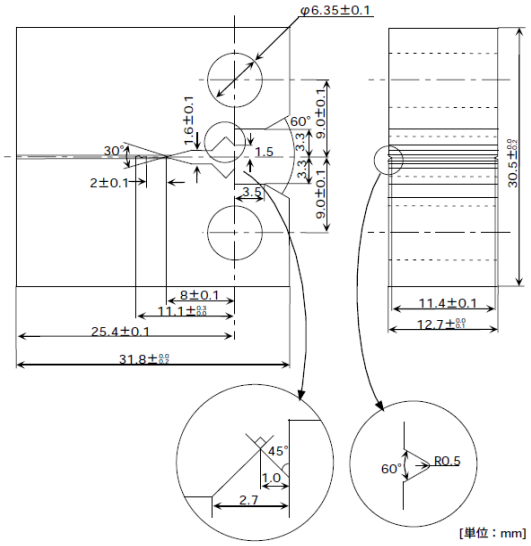

Fig. 1 Geometry and size of CT specimen

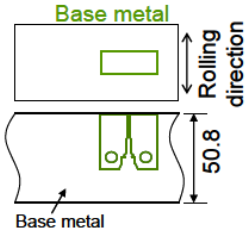

Fig. 2 Sampling position of CT specimen

C. *Irradiation of Specimen*

The specimens were irradiated in the Japan Materials testing Reactor (JMTR) of the Japan Atomic Energy Agency (JAEA) in the high temperature water. The irradiation temperature was 288°C (262-302°C) and the inlet conductivity of the irradiation capsule was kept below 0.1 S/cm during the irradiation. The first neutron fluence of the specimen was ranging from $5x10^{24}$ to $1x10^{26}$ n/m^2 (0.7-14dpa). After irradiation, post irradiation tests (PIEs) have been performed in Nippon Nuclear Fuel Development Co., Ltd (NFD) and JMTR hot laboratory facilities.

D. *Crack Growth Tests*

All of the CGR tests were conducted under the constant load condition in BWR simulated water at 288°C. Test facilities are schematically illustrated in Fig. 3. The load was controlled using a load cell installed inside the autoclave. DO concentration was measured continuously at the inlet and outlet. The crack growth was monitored by the reversing dc potential drop (DCPD) method. Conductivity was maintained <0.1μS/cm at the inlet and <0.2μS/cm at the outlet. The electrochemical corrosion potential (ECP) of the specimen was monitored using an internal Ag/AgC1 reference electrode. Prior to the constant load test, gentle cycling (R=0.7, f=0.1-0.0001 Hz) was introduced during the dissolved oxygen level DO1 (>130mV$_{SHE}$, ~32ppm DO at the inlet) at 288 °C until crack growth exceeded the plastic zone associated with fatigue pre-cracking. In each test run, the CGR data at DO1 level (>130mV$_{SHE}$, ~32ppm DO at the inlet) were acquired first and then the ECP was changed to a lower DO2 level (-200mV$_{SHE}$, ~10 ppb DO at inlet) to examine the effect of ECP on CGR. Crack growth rates in 130mV$_{SHE}$ were calculated over time intervals>100 hours, until crack length increments which were calculated using PDM exceeded 0.1 mm. The anion (SO_4^{2-}, Cl^-, NO_3^-) concentration in the test water during the test was kept less than 5 ppb, respectively. They were measured periodically using ion chromatograph with sampling the inlet and the outlet water. After CGR tests, the specimens were failed by cyclic loading at room temperature in air. The fracture morphology was investigated by digital optical microscopy and scanning electron microscopy (SEM), and the crack length measured by this observation was used to calibrate the DCPD CGR data. The average crack length was obtained by dividing the area of SCC by the width of SCC.

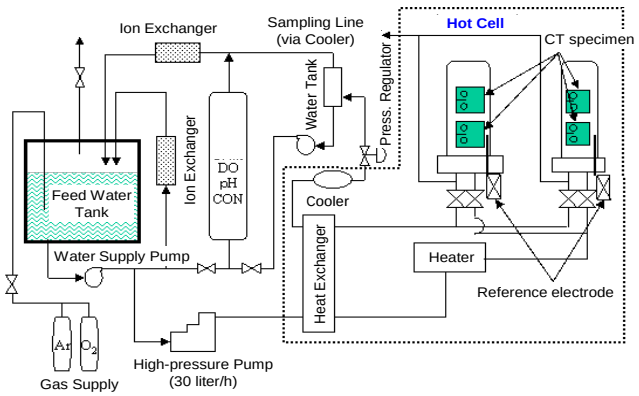

Fig. 3 Schematic of CGR test facilities

III. RESULTS AND DISCUSSION

The CGR data of neutron irradiated Type 304 SS are shown in Table 2. All of the CGRs in this paper were

corrected based on the fracture surface observation. That is, the crack extensions determined from the DCPD measurement were proportionally scaled to match the final optically measured average crack extension length. The test K range was from 12 to 29 MPam$^{1/2}$.

Table 2 CGR test results of Type 304 SS under constant load conditions

Material	ID	B(1) (mm)	Neutron fluence (dpa)	DO (2)	K (MPam$^{1/2}$)	CGR (m/s)
Type 304 SS	R103	12.7	0.62	DO1	20.6	8.00E-11
	R104		0.71	DO1	15.6	7.60E-11
	R303	6.4	4.02	DO1	26.5	1.90E-09
				DO2	28.3	2.70E-10
	R306		3.47	DO1	14.9	5.30E-10
				DO2	15	< 1.0E-11
	R404	5.6	8.6	DO1	11.3	3.70E-10
				DO2	11.6	5.40E-11
	R406		9.2	DO1	15.5	9.60E-10
				DO2	16.2	5.50E-11

(1) Thickness of 0.5T-CT specimen
(2) DO1 (□ 32ppmDO at inlet, Target ECP: >130mVSHE), DO2 (<10ppb DO at inlet, Target ECP: -200mVSHE)

Fig. 4 shows the relationship between crack length and time during pre-cracking under gentle cycling to the constant load for the R303 (304, 2.4x10^{25} n/m^2 (3.4dpa)) specimen. In this case, crack growth constantly under a high-DO environment, CGR=9x10^{-9} m/s was measured and the average K was 26.5 MPam$^{1/2}$ during the estimated period. After the high-DO environment (ECP=140mV$_{SHE}$) testing, we had adjusted the oxygen density and changed the environment to a low-DO condition (ECP=-230mV$_{SHE}$). At the low-DO environment, the crack growth rate immediately decreases below 1.8x10^{-10} m/s. Intergranular cracking was observed in the fracture surface that corresponds to the constant load condition, as shown in Fig. 4. For the A301 (316L, 2.7x10^{25} n/m^2(3.9dpa)) specimen, the beneficial effect of reducing the ECP (ECP reduced from 140 to -230mV$_{SHE}$) on CGR was observed, that is, the CGR reduced from 1.2x10^{-9} m/s to 1.9x10^{-11} m/s, while the average K increased slightly from 11.3 to 11.7 MPam$^{1/2}$ as shown in Fig. 5. Therefore, the beneficial effect of reducing the ECP to below -230mV$_{SHE}$ on the CGR was observed, although this effect showed a tendency to be small with increase of neutron fluence of specimens. Intergranular cracking was observed on the whole fracture surface for Type 304 and L-grade SS irradiated until 1x10^{26} n/m^2 (14dpa).

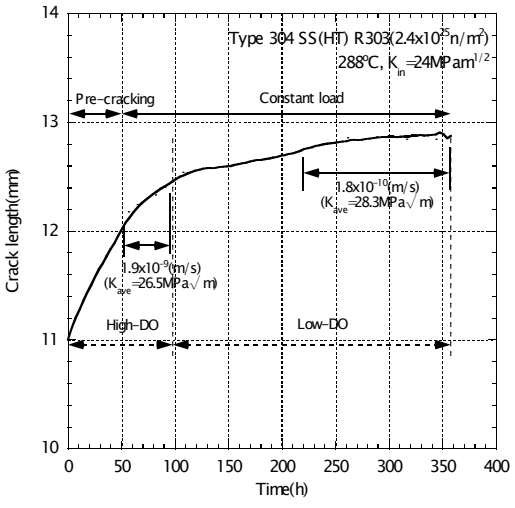

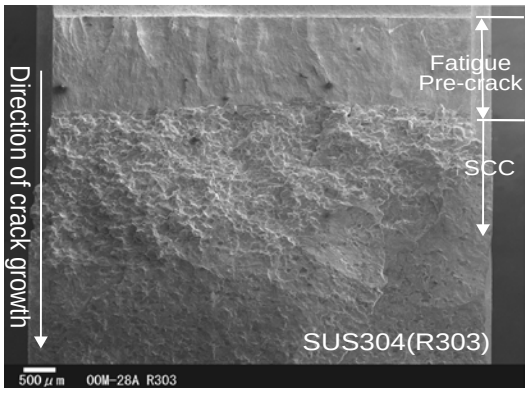

Fig. 4 Crack growth behavior and fracture surface (Type 304 SS)

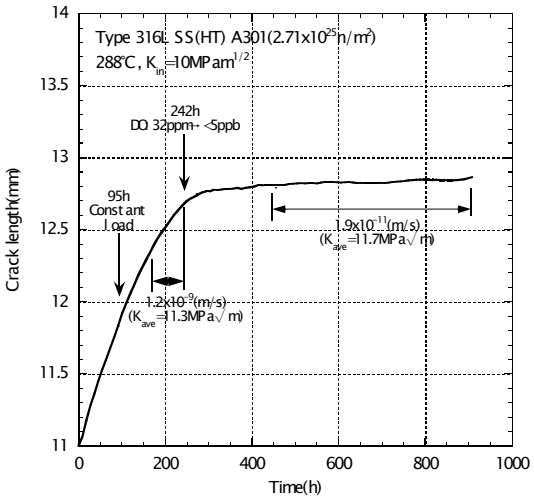

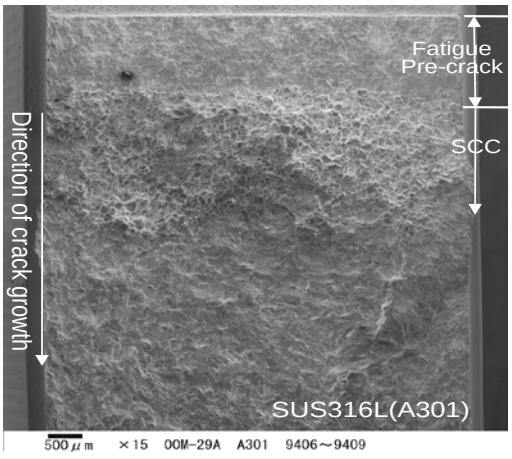

Fig. 5 Crack growth behavior and fracture surface (Type 316L SS)

In the case of Type 304 SS, lineage structure by rolling was observed on the fracture surface. The electron backscattered diffraction pattern (EBSD) observation was conducted on the cross section of Type 304 SS specimen in order to investigate the influence of lineage structure in the rolling process on the CGR behavior. The phase image and kernel average misorientation (KAM) data are shown in Fig. 6. In the phase image, grey shows the austenitic phase and red shows the ferritic phase. Since the local change of KAM was not observed near the ferritic phases, the influence of lineage structure by rolling on the CGR behavior was considered to be small.

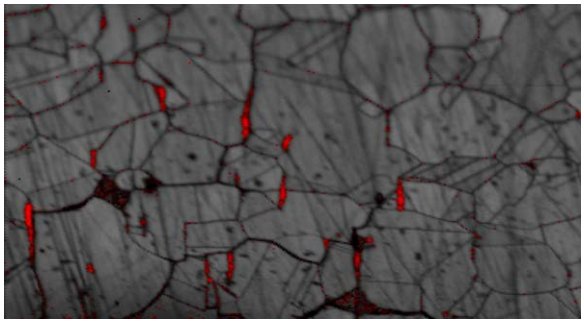

(a) Phase image

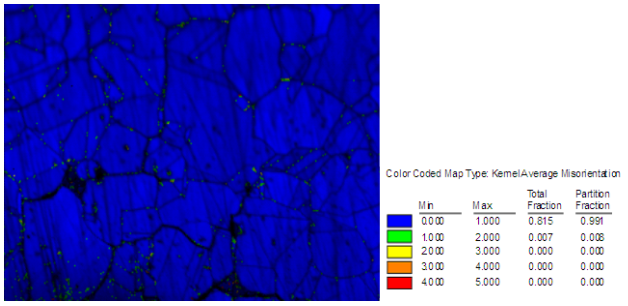

(b) Kernel average misorientation data

Fig. 6 EBSD data of irradiated material

The K dependence of CGR for Type 304 SS in the normal water chemistry (NWC) (ECP=140mV$_{SHE}$) is shown in Fig. 7. The CGR increase with increasing neutron fluence and the power law of K on the CGR was observed above F2 neutron fluence level (>1.0x10^{25} n/m^2 (1.4dpa)) as shown in Fig. 7(a). Fig. 7(b) shows the K dependence of CGR including the CGR data for Type 304L, 316L SS and the literature data [11-14]. The CGR data for Type 304 SS show good agreement with the JSME rules for "Fitness-for-Service" for nuclear power plants. The different tendency is observed between Type 304 SS and L-grade SS (Type 304L and 316L SS) with increasing neutron fluence above F3 (3x10^{25} n/m^2 (4.3dpa)) level.

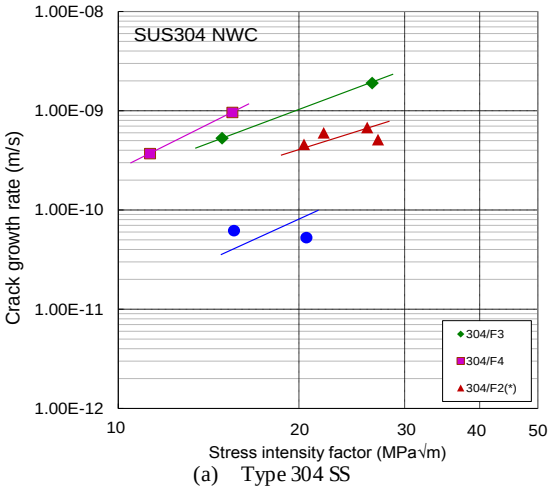

(a) Type 304 SS

Fig. 8 shows the neutron fluence dependence on CGR of Type 304 SS in the NWC condition including Type 304L and 316L SS data. The CGR of Type 304 SS increases with increasing neutron fluence. The CGR of Type 304 SS is slightly smaller than those of Type 304L and 316L SS at the same neutron fluence and reaches to 1.0x10^{-9} m/s in 9dpa.

The CGR of Type 304L and 316L SS saturate in about 2dpa and 4dpa, respectively.

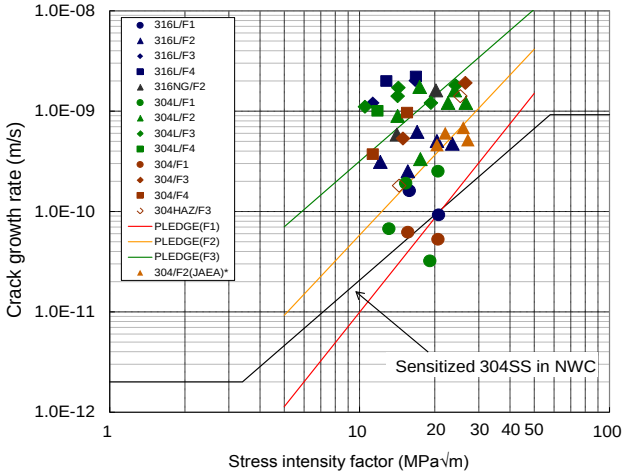

(b) Type 304, 304L and 316L SS

Fig. 7 K dependence on CGR

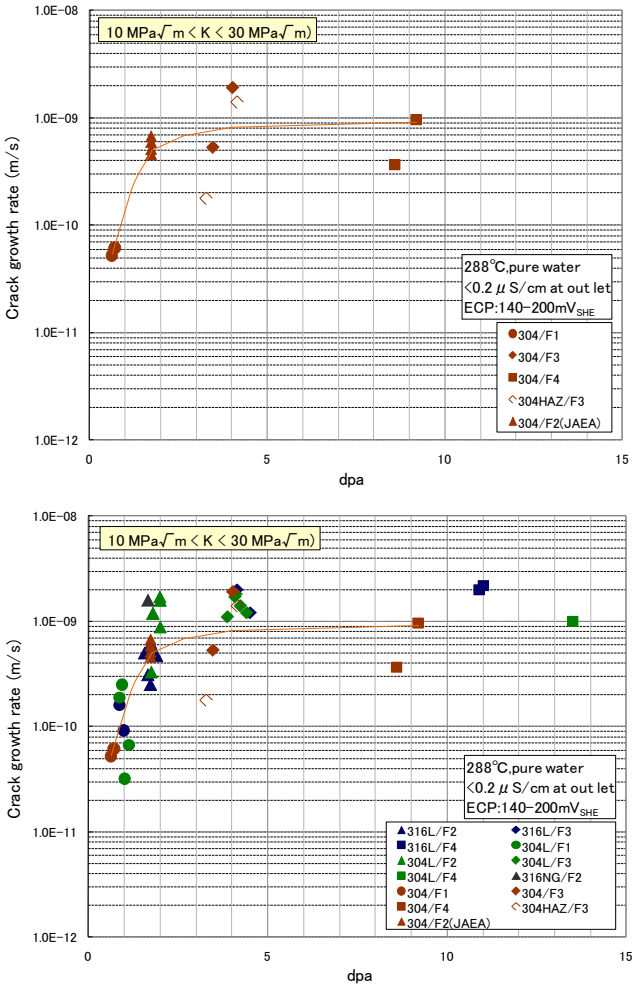

Fig. 8 Neutron fluence dependence on CGR

In order to investigate the influence of radiation hardening on CGR, the tensile tests were conducted for the irradiated materials. The neutron dependence on 0.2 % offset stress and uniform elongation are shown in Fig. 9. As for the neutron fluence dependence on 0.2 % offset stress,

the data of Type 304 SS are larger than that of L-grade SS and the same tendency is observed for all materials. The uniform elongation of Type 304 and 304L SS is almost 0 % at 4dpa, but Type 316L SS shows some uniform elongation above 4dpa. It is implied that the local deformation like channeling deformation of Type 316L SS is dominant in the faster fluence level than that of Type 304L SS. This tendency shows good agreement with the neutron fluence dependence on CGR for Type 304L and 316L SS. Fig. 10 shows the relationship between increase in hardness caused by irradiation and CGR. The CGR increases with increasing hardness for all materials. The tendency for Type 304 SS is slightly different from that of Type 304L and 316L SS in the lower neutron fluence region.

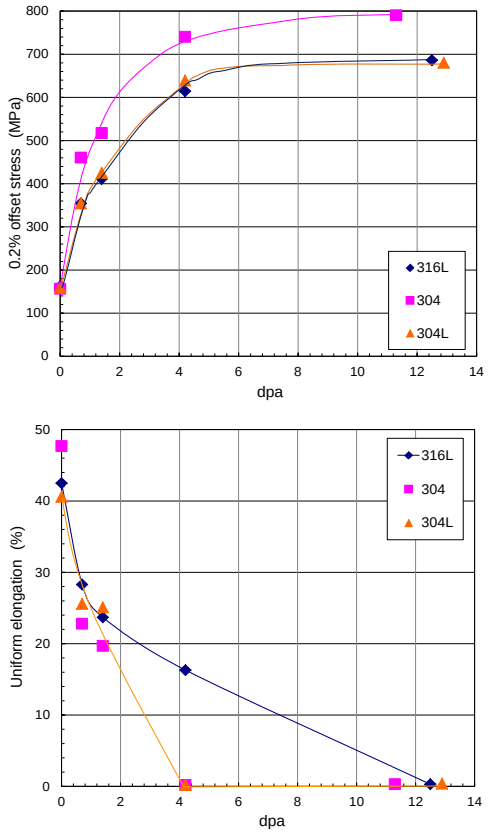

Fig. 9 Neutron fluence dependence on 0.2 % offset stress and uniform elongation

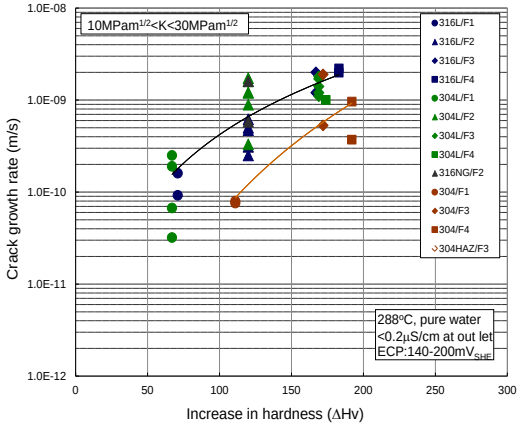

Fig. 10 Relationship between hardness and CGR

In order to understand the characteristics of CGR from the viewpoint of RIS, neutron dependence of the deviation in chromium, nickel, silicon and phosphorus concentrations at the grain boundary from the bulk of irradiated materials are shown in Fig. 11. In this figure, Cr (base) is the bulk composition in the each neutron fluence level condition. The chromium depletion at a grain boundary increases with increasing neutron fluence. On the other hand, the enrichment of nickel and silicon at a grain boundary increase with increasing neutron fluence. The grain boundary concentration of phosphorus does not show distinct segregation. There is no difference on the neutron fluence dependence of RIS for all irradiated materials. The relationship between change of chromium depletion and CGR is shown in Fig. 12. Although the CGR increases with increasing chromium depletion at a grain boundary, the CGR is not coincided with change of chromium depletion for all materials in high neutron fluence region.

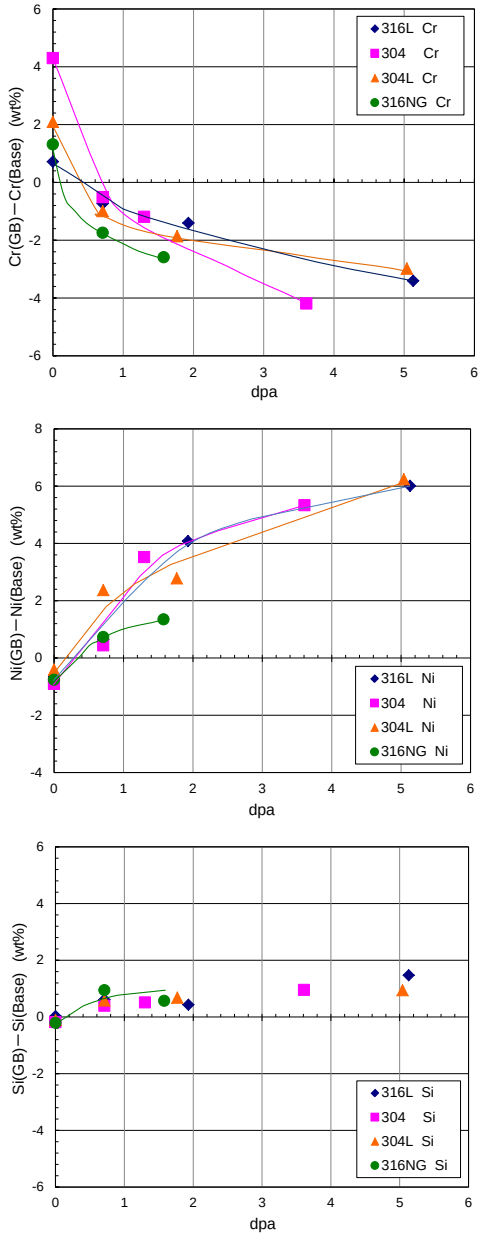

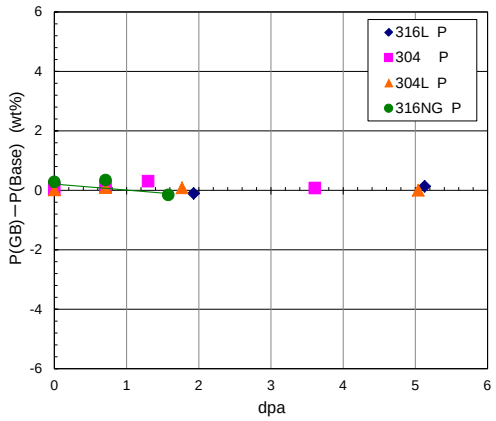

Fig. 11 Neutron fluence dependence on RIS

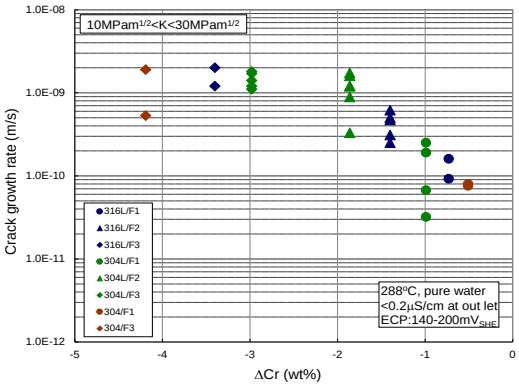

Fig. 12 Relationship between RIS and CGR

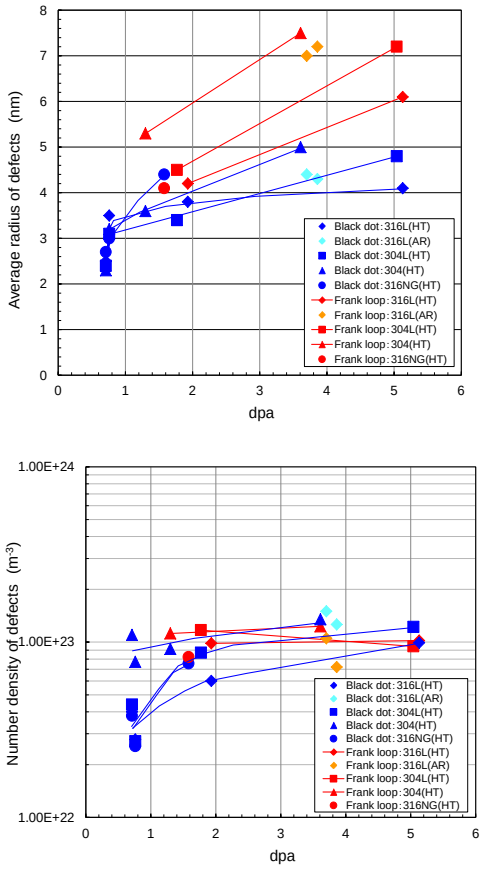

Fig. 13 Neutron fluence dependence on microstructure

Fig. 13 shows neutron fluence dependence on microstructures for all irradiated materials. Although there is no difference on the number density of dislocations for all materials, the average radius of dislocations for Type 304 SS is larger than that of l-grade SS and this tendency is coincide with the neutron dependence on 0.2 % offset stress.

IV. CONCLUSION

The CGR tests of neutron irradiated Type 304 SS were conducted in BWR conditions and the results were compared with those of Type 304L and 316L SS, and following results were obtained.

(1) The CGR increases with increasing neutron fluence and the power law of K on the CGR was observed above F2 neutron fluence level ($1.0x10^{25}n/m^2$ (1.4dpa)). The different tendency is observed between Type 304 SS and L-grade SS (Type 304L and 316L SS) with increasing neutron fluence above F3 ($3x10^{25}$ n/m^2 (4.3dpa)) level.

(2) The CGR of Type 304 SS is slightly small as compared with those of Type 304L and 316L SS at the same neutron fluence and shows an increasing tendency above 4 dpa and reaches to $1.0x10^{-9}$ m/s in 9dpa.

(3) The neutron fluence dependence on uniform elongation is different with Type 304, 304L SS and Type 316L SS. That is, the neutron fluence in which the local deformation like channeling deformation is dominant, high for Type 316L SS. The 0.2 % offset stress and Vickers hardness of Type 304 SS are slightly larger than those of L-grade SS.

(4) There is almost no difference in the composition analysis around grain boundary with Type 304, 304L and 316L SS.

(5) The average radius of microstructures for Type 304 SS shows slightly bigger tendency as compared with that of L-grade SS.

ACKNOWLEDGMENTS

The experiments and analysis for the L-grade SS were mainly conducted in the Toshiba Corp., the Hitachi-GE Nuclear Energy Co., Ltd and the NFD. The authors express their sincere thanks to the Toshiba Corp., the Hitachi-GE Nuclear Energy Co., Ltd and the NFD for supporting the experiments. This work was performed as a part of the IASCC project "Evaluation Technology for Irradiation Assisted Stress Corrosion Cracking" supported by the Ministry of Economy, Trade and Industry (METI).

REFERENCES

[1] W. L. Clarke and A. J. Jacobs, "Effect of Radiation Environment on SCC of Austenitic Materials", Proceedings of First International Symposium on Environmental Degradation of Materials in Nuclear Power System Water Reactors, Myrtle Beach, South Carolina, August 1983, 451-461.

[2] F. Garzarolli et al., "Deformability of Austenitic Stainless Steels and Ni base Alloys in the Core of a Boiling and a Pressurized Water Reactor", Proceedings of Third International Symposium on Environmental Degradation of Materials in Nuclear Power System Water Reactors, Traverse City, Michigan, September 1987, 657-664.

[3] A. J. Jacobs et al., “Radiation Effects on the Stress Corrosion and Other Selected Properties of Type 304 and Type 316 Stainless Steels”, ibid., September 1987, 673-680.

[4] A. J. Jacobs and G. P. Wozadlo, “Irradiation Assisted Stress Corrosion Cracking a Factor in Nuclear Power Plant Aging”, Proceedings of International Conference on Nuclear Power Plant Aging Availability Factors and Reliability Analysis, ASM, 1985, 173-182.

[5] D. I. R. Norris, C. Baker, and J. M. Titchmarsh, “Compositional Profiles at Grain Boundaries in 20%Cr/25%Ni/Nb Stainless Steel”, Proceedings of Symposium on Radiation Induced Segregation of Stainless Steel held at Berkeley Nuclear Laboratory, CEGB, September 1986, 86-98.

[6] H. Hanninen and Aho Mantina, “Environment Sensitive Cracking of Reactor Internals”, Proceedings of Third International Symposium on Environmental Degradation of Materials in Nuclear Power System Water Reactors, Traverse City, Michigan, September 1987, 77-92.

[7] P. L. Andersen et al., “State of Knowledge of Radiation Effects on Environmental Cracking in Light Water Reactor Core Materials”, Proceedings of Fourth International Symposium on Environmental Degradation of Materials in Nuclear Power System Water Reactors, Jekyll Island, Georgia, August 1989, 83-121.

[8] M. Kodama et al., “Effects of Fluence and Dissolved Oxygen on IASCC in Austenitic Stainless Steels”, Proceedings of Fifth International Symposium on Environmental Degradation of Materials in Nuclear Power System Water Reactors, Monterey, California, August 1991, 948-954.

[9] K. Chatani et al., “IASCC Crack Growth Rate of Neutron Irradiated Low Carbon Austenitic Stainless Steels in Simulated BWR Condition”, Proceedings of 13th International Symposium on Environmental Degradation of Materials in Nuclear Power Systems-Water Reactors, August 2007.

[10] K. Takakura, K. Nakata, “IASCC Crack Growth Behavior of Neutron Irradiated Stainless Steels”, Proceedings of the International Symposium on Research for Aging Management of Light Water Reactors, October 22-23, 2007, Fukui City, JAPAN.

[11] Codes for Nuclear Power Generation Facilities -Rules on Fitness-for-Service for Nuclear Power Plants-, JSME S NA1-2004(2004).

[12] S. Ooki, Y. Tanaka, K. Takamori, S. Suzuki, S. Tanaka, Y. Saito, T. Nakamura, T. Kato, K. Chatani and M. Kodama, “Study on SCC Growth Behavior of BWR Core Shroud”, Proceedings of 12th Int. Conf. Environmental Degradation of Materials in Nuclear Systems- Water Reactors, August 2005.

[13] O. K. Chopra, E. E. Gruber and W. J. Shack, “Crack Growth Behavior of Irradiated Austenitic Stainless Steels in High-Purity Water at 289^{o}C”, Proceedings of 11th Int. Symp. on Environmental Degradation of Materials in Nuclear Power Systems- Water Reactors, August 2003.

[14] Y. Kaji, H. Ugachi, T. Tsukada, J. Nakano, Y. matsui, K. Kawamata, A. Shibata, M. Ohmi, N. Nagata, K. Dozaki and H. Takiguchi, “In-Core SCC Growth Behavior of Type 304 Stainless Steel in BWR Simulated High-Temperature Water at JMTR”, Journal of Nuclear Science and Technology, Vol.45, No.8, 2008, 725-734.